



IJPPR

INTERNATIONAL JOURNAL OF PHARMACY & PHARMACEUTICAL RESEARCH
An official Publication of Human Journals

ISSN 2349-7203



Human Journals

Research Article

August 2018 Vol.:13, Issue:1

© All rights are reserved by Marwa Donia et al.

Acetazolamide Nanosuspension: Influence of Process and Formulation Variables on Particle Size Reduction and Dissolution Enhancement



ISSN 2349-7203

IJPPR
INTERNATIONAL JOURNAL OF PHARMACY & PHARMACEUTICAL RESEARCH
An official Publication of Human Journals



**Marwa Donia^{*}, Rihab Osman, Gehan A.S. Awad,
Nahed Daoud Mortada**

*Faculty of Pharmacy, Ain Shams University, P.O. Box
11566, Cairo, Egypt.*

Submission: 20 July 2018
Accepted: 27 July 2018
Published: 30 August 2018

Keywords: Nanosuspension; Saturation solubility; Acetazolamide, poorly soluble drug; Nanoprecipitation

ABSTRACT

The objective of this study was to prepare nanosuspension (NS) of a poorly soluble anti-glaucoma drug, acetazolamide (ACZ) adopting the antisolvent precipitation (AS-PT) coupled with the sonication technique. Using a systematic one factor at a time experimental design, various process and formulation variables were optimized to ensure a uniform small particle size around 100 nm. Using ACZ concentration of 50mg/mL, solvent antisolvent ratio of 1:50 and polyvinyl alcohol (PVA) as the polymeric stabilizer; the obtained ACZ-NS scored a PS of 117.4 ± 11.1 nm and PDI of 0.29 ± 0.04 . Spherical particles were visualized using TEM and proved to be amorphous by DSC analysis. NS was successfully prepared with remarkable enhancement of dissolution rate compared to untreated ACZ.



www.ijppr.humanjournals.com

INTRODUCTION

Nanosuspension (NS) has emerged as one of the leading approaches for enhancement of solubility of poorly soluble drugs which represent about 40% of the marketed products and about 70-90% of the new drug candidates[1]. It is defined as a colloidal dispersion of pure drug particles below 1 μ m surrounded by surfactant (SAA) or polymer stabilizer or a combination of both [2]. Representing drug particles only, NS offers several advantages over other nano drug delivery systems. NS enhances the dissolution rate and saturation solubility of poorly water and oil soluble drugs excluding the need for organic solvents [3]. Moreover, it enhances particles permeability through increased adhesiveness [4]. Furthermore, nanocrystals of PS below 100nm nominated as smart crystals since they show altered physical properties and cellular uptake behavior; interesting properties in case of parenteral delivery for targeting specific cells or decreasing side effects [5]. All these reasons were behind the approval of many marketed NS products as Rapamune[®], Emend[®] and Megace[®] [6]. Noteworthy to mention that, Rapamune[®] appeared only after 10 years of technology innovation confirming industrial feasibility and easy scaling up of this rapidly growing technology[6].

Two techniques are widely used for NS production: top-down or bottom-up. The former involves the degradation of large drug particles into a smaller one by different milling techniques as high-pressure homogenizer (HPH) and media milling [7, 8]. In spite of the industrial feasibility of this technique, it can result in chemical degradation, metal impurities with limited size reduction [9]. Conversely, the bottom-up technique provides less expensive, simple, low-temperature process suitable for thermo-labile drugs. Unfortunately, it requires strict control over numerous conditions that strongly affect the final PS and cost of organic solvents removal. Antisolvent precipitation coupled with sonication is a common technique for NS production[10, 11].

Acetazolamide (ACZ) is a *carbonic anhydrase* inhibitor; used in the treatment of glaucoma when administered as oral tablets, capsules, and IV solution [12]. However, Side effects like diuresis and metabolic acidosis limit the usefulness of this drug. Unfortunately, ACZ is a BCS (biopharmaceutical classification system) class IV drug; has poor aqueous solubility (0.7mg/mL) and low permeability coefficient of (4.11x10⁻⁶cm/s) that limits its ocular bioavailability [13].Ocular delivery of ACZ is expected to decrease side effects and enhance patient compliance. High tear turns over, low dose volume, nonproductive absorption through

the conjunctiva and nasolacrimal duct and corneal poor permeability with tight junctions are some of the barriers that should be overcome while designing a drug for ocular delivery [14].

ACZ had been fabricated as liposomes, niosomes, dendrimers, nanocapsules and other topical dosage forms [13-16]. To the authors' knowledge, the NS of ACZ had not been addressed in previous articles. Accordingly, the purpose of this study was to formulate topical ACZ-NS using AS-PT technique with optimum PS that provides high water solubility and corneal permeability. Special focus will be given to the various process and formulation factors affecting the size and stability of the NS using various stabilizers.

MATERIALS AND METHODS

1.1. Materials

Acetazolamide (ACZ): kindly provided by Chemical Industries Development (CID) company, Cairo, Egypt. Polyvinyl alcohol (PVA): viscosity 25 to 32cP, LOBA CHEMIE, Mumbai, India. Poloxamer 407 (P-407): SERVA Electrophoresis GmbH, Heidelberg. DMSO: SDFCL, Mumbai-30, India.

1.1. Experimental design

ACZ-NS was fabricated *via* the previously described anti-solvent precipitation (AS-PT) method [10, 17]. The method was based on rapidly injecting ACZ dissolved in the solvent (S), DMSO, into an antisolvent (AS), water, containing a stabilizer and placed on a magnetic stirrer (Ika magnetic stirrer with heater, MAG HS7, Wilmington, USA) at a specified speed on an ice bath (5°C). The whole dispersion was then subjected to sonication by either bath (Model 275T, Crest ultrasonic ETL testing laboratories, Cortland, NY) or probe sonicator (Crest ultrasonic ETL testing laboratories, Cortland, NY) for a predetermined time. The effect of various experimental and formulation variables on the characteristics of the prepared ACZ-NS was evaluated. The compositions of the prepared formulae and the process factors studied are shown in Table 1.

Table 1: Tested factors and compositions of ACZ-NS formulae prepared by the AS-PT method.

| | Factor | Formula code | Stirring | | Sonicator | | Stabilizer | | ACZ Conc./S (mg/mL) | S/AS ratio | | |
|----------------------|-------------|--------------|------------|------------|-----------|------------|------------|------------|---------------------|------------|-----|------|
| | | | Rate (rpm) | Time (min) | Type | Time (min) | Type | Conc. %w/v | | | | |
| Experimental factors | Stirring | F1 | 500 | 15 | (A*) | 45 | PVA | 0.1 | 20 | 1:50 | | |
| | | F2 | | 30 | | | | | | | | |
| | | F3 | 1000 | 15 | | | | | | | | |
| | | F4 | | 30 | | | | | | | | |
| | | F5 | 1500 | 15 | | | | | | | | |
| | | F6 | | 30 | | | | | | | | |
| | Sonication | F7 | 1000 | 15 | (A*) | 15 | | | | | | |
| | | F8 | | | | 30 | | | | | | |
| | | F9 | | | | 45 | | | | | | |
| | | F10 | | | | 60 | | | | | | |
| | | F11 | | | | (B**) | | | | | 15 | |
| | | F12 | | | | | | | | | 30 | |
| | 45 | | | | | | | | | | | |
| Formulation factors | S /AS ratio | F3 | | | 1000 | 15 | (A*) | 45 | P-407 | 50 | 20 | 1:50 |
| | | F13 | | | | | | | | | 35 | 1:30 |
| | | F14 | | | | | | | | | 50 | 1:10 |
| | ACZ Conc. | F3 | | | | | | | | | 75 | 1:50 |
| | | F15 | | | | | | | | | 100 | |
| | | F16 | 0.1 | | | | | | | | | |
| | | F17 | 0.2 | | | | | | | | | |
| | | F18 | 0.4 | | | | | | | | | |
| | Stabilizer | F16 | 1:50 | 0.1 | | | | | | | | |
| | | F19 | | 0.2 | | | | | | | | |
| | | F20 | | 0.4 | | | | | | | | |
| | | F21 | | 0.1 | | | | | | | | |
| F22 | | 0.2 | | | | | | | | | | |
| F23 | | 0.4 | | | | | | | | | | |

*(A): bath sonication operated at maximum power, *(B): probe sonication operated at 100% power (24KHz). ACZ: acetazolamide, PVA: polyvinyl alcohol, P-407: poloxamer 407, S/AS: solvent to anti-solvent ratio.

2. Characterization of ACZ-NS

2.1. Particle size (PS) and polydispersity index (PDI) determination

Malvern Zetasizer 4 Nano series (Malvern Instruments Ltd, Malvern, UK) was used to measure the hydrodynamic diameter (Z- average) and PS distribution expressed as the polydispersity index (PDI) of ACZ-NS formulae using dynamic light scattering technique (DLS). Freshly prepared formulae were placed in disposable polystyrene cells, the PS expressed as intensity and PDI were measured at 25°C. The measurement was made in triplicates.

2.2. Microscopical examination

2.2.1. Transmission electron microscopy (TEM)

The selected ACZ-NS formula was visualized using (TEM) (JEM-2100, Joel, Tokyo, Japan). One drop of the NS was added to a carbon-coated copper grid followed by coating with 2% w/v phosphotungstic acid. The equipment was operated at power 200 kV[1].

2.2.2. Optical microscopy

Micrographs of drug crystals and selected ACZ-NS were visualized using an optical microscope (Carl Zeiss Axiostar plus, Transmitted-Light Microscope, Germany). Slides were prepared by sprinkling powder on the slide with drops of water. The slides were topped with coverslips using magnification lens 40X.

2.3. Differential scanning calorimetry (DSC)

Thermal behavior of ACZ, PVA, and the final selected formula was studied using (DSC-60plus, Shimadzu, and Tokyo, Japan). The equipment, calibrated with indium, was operated under a nitrogen gas flow rate of 20-30 mL/min and heating rate of 10°C/ min. The sample, weighs 1-3 mg, was added to sealed standard aluminum pans and heated from 30 to 300°C.

2.4. ACZ *in vitro* release study

An accurately measured volume equivalent to 1.5mg ACZ was taken from the selected formulation and drug suspension prepared at the same concentration and was transferred to a bottle containing 25mL PBS pH 7.4 achieving sink condition [18, 19]. The temperature was

kept constant at 37 ± 0.5 °C in a shaking water bath (GFL1083, THERMOLAB[®], Burgwedel, Germany) rotating at 50 strokes/min. At specified time intervals: 5, 15, 30, 45 and 60 min, 1mL sample was withdrawn from dissolution medium and was replaced with fresh buffer. Finally, the withdrawn samples were filtered through a $0.22\mu\text{m}$ filter and were analyzed using spectrophotometer at λ_{max} 266nm to determine ACZ content [20]. The experiment was made in triplicates.

3. Data statistical analysis

All results are expressed as the mean of three determinations \pm standard deviation (s.d.). Student's t-test was used when comparing two groups while one-way analysis of variance (ANOVA) was applied when comparing more than two groups along with Tukey's multiple comparison tests as a post hoc test. The probability of error was selected ($P < 0.05$) in all experiments. A trial version of Graph Pad Prism5 program was used during the whole study.

RESULTS AND DISCUSSION

The ultimate goal of this study was to prepare ACZ-NS suitable for ocular delivery. The dispersed particles should possess uniform particle size (PS) in the range of 100-300nm with good saturation solubility. In spite of its ease and low cost, AS-PT method requires strict control over many factors affecting nucleation and crystal growth. Comes in the first place, selection of a good solvent for ACZ: a solvent providing high initial drug concentration will ensure high supersaturation defined as the ratio of particle solubility at the interface (C_s) to bulk solubility (C_∞) [21]. At high supersaturation levels, the nucleation process is rapid and homogenous, giving small initial nuclei size, that continues until supersaturation depletion. The nuclei will continue growing up until reaching a critical size resistant to dissolution [21]. It has been previously reported that DMSO is the best organic solvent for ACZ [22]. It can thus provide a high supersaturation with consequent fast nucleation. Furthermore, DMSO is considered a class III solvent with low toxicity and risks to human health according to the International Conference on Harmonization (ICH) [23]. Due to its low aqueous solubility, water was selected as AS for ACZ NS preparation [22]. Increased temperature usually increases drug bulk solubility decreasing the supersaturation ratio [24]. Besides, temperature elevation accelerates also the rate of diffusion as well as the reaction kinetics at the particle boundary layer, facilitating particle growth and Ostwald ripening [25]. Furthermore, with increasing temperature, the solution viscosity decreases provoking particle collision,

aggregation, and agglomeration followed by further particle growth [26]. Thus, and following a preliminary study the temperature was controlled at 5°C using an ice bath throughout NS preparation. Adjusting these conditions, while varying other parameters, tables 2 and 3 show the characterization of the prepared formulae using different experimental and formulation variables.

4.1.Preparation and optimization of ACZ-NS

4.1.1. Effect of stirring rate and time

Table 2 and figure 1 depict that, at a fixed stirring time (15min), a significant ($P < 0.0001$) decrease in PS was evident by increasing stirring rate from 500rpm (F1) to 1000rpm (F3). Conversely, a further increase to 1500rpm in F5 led to significant ($P < 0.0001$) increase in PS. The PDI showed the non-significant difference between F1 and F3 ($P > 0.05$). However, a significantly higher PDI was seen in F5 ($P < 0.0001$). Similarly, stirring time increase from 15 to 30min at 500rpm had a reducing effect on PS as could be seen by comparing F2 to F1 with respective PS of 182.5 ± 28.3 and 312.5 ± 44.4 nm. On the other hand, prolonging stirring time to 30min at 1000rpm caused no significant effects ($P > 0.05$) on both PS and PDI. Sufficient mixing is required to get a critical supersaturation concentration that triggers homogenous nucleation, producing small-sized nuclei and uniform PS distribution [9]. According to Murnane and *co-workers*, two-time scales described precipitation, time of mixing and time of precipitation. Time of mixing includes either micromixing due to diffusion or mesomixing (interaction of particles together) due to turbulence. Micromixing is increased by accelerating stirring speed, facilitating solvent diffusion and decreasing the thickness of the stagnant boundary layer, Thus, nucleation rate increases and small nuclei are obtained. Further increase in stirring speed, beyond a critical value, or longer stirring time, may induce turbulence that triggers mesomixing. Hence, local supersaturation and nucleation rate decrease, enhancing PS enlargement with a wide size distribution [27]. Therefore, it appeared that stirring at 1000rpm for 15 min was optimum to produce the smallest PS seen with F3.

Table 2: Effect of experimental variables on the PS and PDI of ACZ-NS

| Formula code | Stirring rate (rpm) | Stirring time (min) | Sonication | | PS (nm) | PDI | |
|--------------|---------------------|---------------------|------------|------------|----------------|---------------|-----------|
| | | | type | time (min) | | | |
| F1 | 500 | 15 | A | 45 | 312.50 ± 44.40 | 0.38 ± 0.01 | |
| F2 | | 30 | | | 182.50±28.30 | 0.28±0.03 | |
| F3 | 1000 | 15 | | | 146.30±14.60 | 0.35±0.04 | |
| F4 | | 30 | | | 204.70±35.20 | 0.28±0.03 | |
| F5 | 1500 | 15 | | | 386.05±59.60 | 0.62±0.07 | |
| F6 | | 30 | | | 376.30±54.50 | 0.44±0.03 | |
| F7 | 1000 | 15 | | 15 | 365.50±15.10 | 0.40±0.05 | |
| F8 | | | | 30 | 326.30±33.60 | 0.40±0.04 | |
| F9 | | | | 60 | 430.90±59.70 | 0.48±0.08 | |
| F10 | | | | B | 15 | 281.50±63.50 | 0.39±0.07 |
| F11 | | | | | 30 | 870.90±114.60 | 0.78±0.01 |
| F12 | | | | | 45 | 2221±253.10 | 1.00±0.00 |

All formulae contained 20mg/mL ACZ and 0.1% w/v PVA solution as a stabilizer; S/AS ratio was 1:50, using A bath sonication; B probe sonication both at 5 °C.

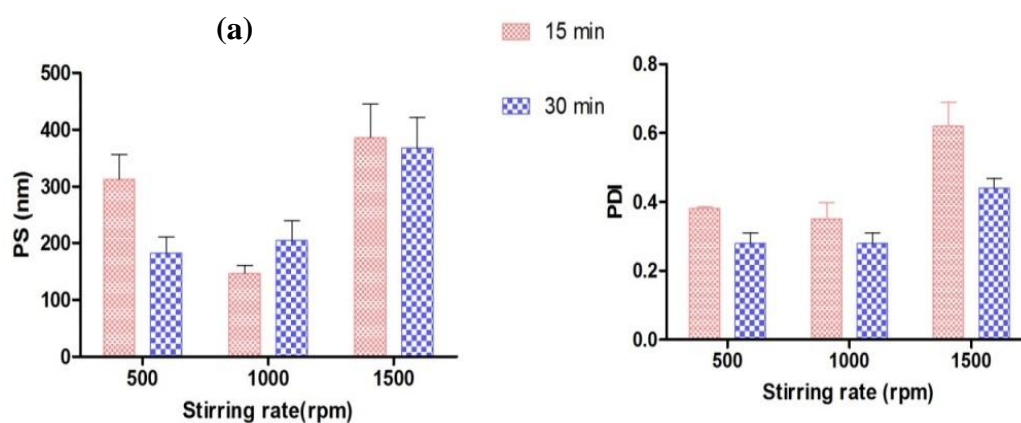


Figure 1: Effect of stirring rate for different time intervals on (a) PS and (b) PDI of ACZ-NS.

4.1.2. Effect of sonication type and time

F3, ACZ-NS scoring the smallest PS, did not exhibit the lowest PDI. Accordingly, bath sonication time was modulated. Besides, probe sonication at 100% power was also tried for different time durations. It is evident from table 2 and figures 2 that, decreasing bath sonication time from 45min in F3 to 15 or 30min in F7 and F8, respectively, or increasing it to 60min (F9) caused significant increases in PS to the respective values 365.5 ± 15.1 , 326.3 ± 33.6 and 430.9 ± 59.7 nm ($P < 0.0001$). In addition, the formulation homogeneity diminished as all the PDI were significantly higher than F3 ($P < 0.0001$). Hence, bath sonication for 45min was sufficient to get the least PS and PDI. Sonication was used as a high energy process in combination with AS precipitation for NS preparation [18, 28]. Using ultrasonic waves creates cycles of compression and rarefaction (expansion) that lead to cavitation with the formation of tiny water vapor bubbles. The collapse of these bubbles induces shock waves with a velocity higher than that of sound. This velocity increases micromixing during PT and induces nucleation at lower supersaturation causing PS decrease [9]. Further energy input by increasing amplitude or sonication time beyond a critical value, increases the kinetic energy of the particles inducing particles collisions and agglomeration producing larger PS [26, 29].

Probe sonicator devices are recognized with their higher localized intensity compared to bath sonication. Therefore, they impart a highly efficient sonication process in less time. Probe sonication (B) was applied for 15, 30 and 45min. However, unfortunately, no PS reduction was noticed even at 45min as observed in formulae F10, F11 and F12, respectively. In this system, the probe sonication had induced intense energy; which was not compensated enough by the formulation parameters and also had increased particles collisions thus led to particle aggregation and growing by the time [30].

Although, formula F3 scored the least PS of 146.3 ± 14.6 nm, yet it exhibited a bimodal PS chart, figure 3. The smallest peak was below 100nm and the largest one was around 500 nm. Ostwald ripening of highly energetic different-sized nanoparticles would have occurred [31]. Hence, optimizing the PS distribution was set as a goal in the subsequent studies.

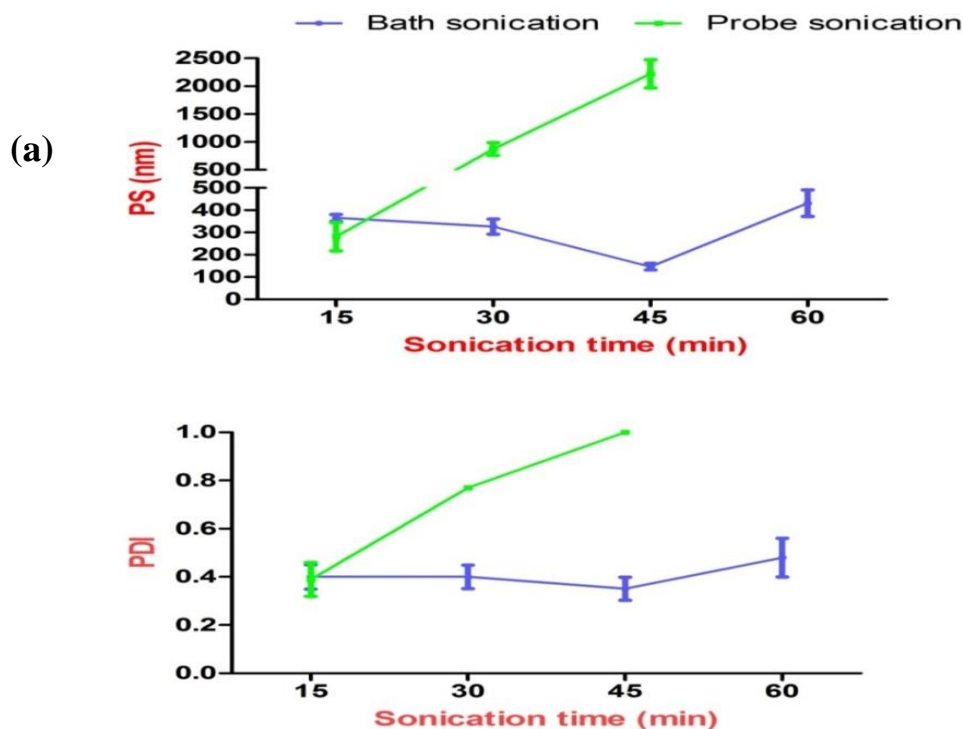


Figure 2: Effect of sonication time (bath/probe) on (a) PS and (b) PDI of ACZ-NS.

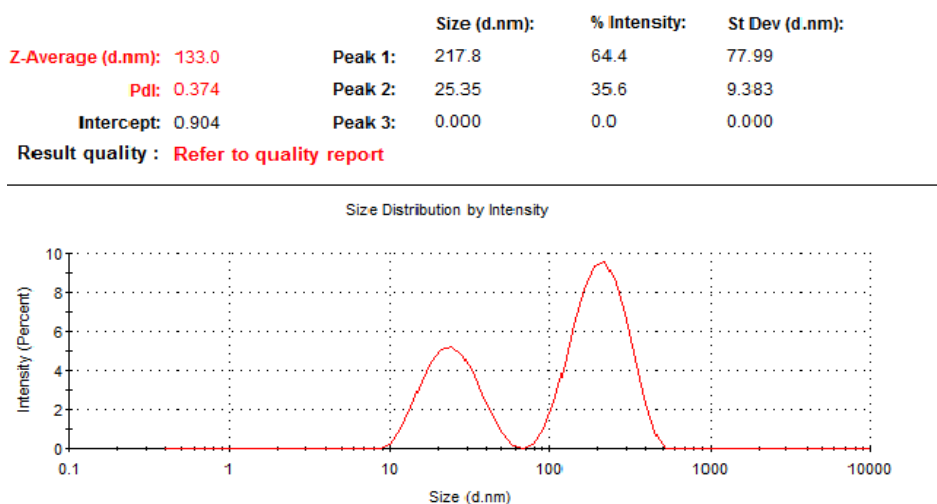


Figure 3: Particle size distribution plot of formula (F3)

Formulation variables

The experimental conditions were set at a stirring rate of 1000 rpm for 15 min followed by bath sonication for 45 min. Uniformity of PS and their distribution (PSD) was tackled in this section by formulation variables. The strategy was to increase the supersaturation ratio by

altering the S/AS ratios or to increase drug concentration in S. We also tried to induce more system stabilization by increasing PVA concentrations or by using another stabilizer.

4.1.3. Effect of the solvent antisolvent ratio (S/AS)

The S/AS ratio was increased by decreasing the volume of AS (0.1% w/v PVA) from 50mL in F3 to 30 and 10mL in F13 and F14, respectively. Table 3 and figure 4 show a significant increase in PS ($P < 0.001$) as S/AS ratio was increased from 1:50 (F3) to 1:30 (F13) and 1:10 (F14). Similarly, significant increases in PDI occurred: from 0.35 ± 0.04 in F3 to 0.47 ± 0.07 and 0.52 ± 0.09 in F13 and F14, respectively.

At critical S/AS ratio, an equilibrium is set between nucleation and growth kinetics, producing optimum PS [9]. The increase in AS volume by decreasing S/AS ratio decreases supersaturation due to drug concentration lowering and PS is expected to increase. Surprisingly, at high S/AS ratio, the high solvent concentration increased drug solubility and particle growth by Ostwald ripening [26]. Similarly, Ying Lu and co-workers had prepared paclitaxel nanocrystals using different S/AS ratios; 1:5, 1:20 and 1:40; the least PS was produced by the ratio 1:20 [17]. Based on the outcome of this study, a 1:50 S/AS ratio will be used. Lower S/AS ratios were not tested due to the high dilution of the drug and the large volume of AS needed.

4.1.4. Effect of ACZ concentration

In an attempt to increase the drug content of NS, ACZ concentration in DMSO was increased from 20 mg/mL in F3 to 35, 50, 75 and 100mg/mL in formulae F15, F16, F17, and F18, respectively. The results in table 3 and figure 5 reveal a concentration-dependent PS increase with increasing ACZ concentration until 75mg/mL. The higher concentration produced immediate drug precipitation (F18). PDI value showed a non-significantly increase ($P > 0.05$) with increasing drug loading. Increasing drug concentrations enhances supersaturation and nucleation rate with the formation of small-sized particles. On the other hand, at high levels of supersaturation too many nuclei are formed, rising the solution viscosity which in turn will lower the diffusion rate of particles and also increase particles collision rate inducing particles aggregation and agglomeration [9, 32]. Theoretically, at very low drug concentration, supersaturation and nucleation rate are decreased producing also large-sized particles. So, optimum drug concentration should be finely tuned to obtain the required PS [26]. In this context, Kumar and co-workers had prepared itraconazole NS and investigated

the drug concentration effect on NS PS. Drug concentration was increased from 10 to 200 and 105 mg/mL was the middle value in a cubic centered design. The smallest PS of 102nm was seen with the lowest drug concentration of 10mg/mL [33]. Similar results were observed in previously published research papers investigating the effect of drug concentration on an organic solvent on PS of the prepared NS [10, 17, 34].

Accordingly, F16, prepared with 50mg/mL seemed to be suitable for more PS modulation. It contains drug amounts sufficiently lower than the precipitating concentration, avoiding particle aggregation.

Table 3: Effect of formulation variables on PS and PDI of ACZ-NS.

| Formula code | S/AS ratio | ACZ conc. (mg/mL) | Stabilizer | | PS (nm) | PDI | | |
|--------------|------------|-------------------|------------|--------------|--------------|-----------|----------------|-----------|
| | | | Type | Conc. (%w/v) | | | | |
| F3 | 1:50 | 20 | PVA | 0.1 | 146.30±14.60 | 0.35±0.04 | | |
| F13 | 1:30 | | | | 297.10±74.70 | 0.47±0.07 | | |
| F14 | 1:10 | | | | 365.60±89.20 | 0.52±0.09 | | |
| F15 | 1:50 | 35 | | | 260.20±27.20 | 0.38±0.03 | | |
| F16 | | 50 | | | 314.60±28.50 | 0.39±0.02 | | |
| F17 | | 75 | | | 441.30±64.10 | 0.37±0.04 | | |
| F18 | | 100 | | | ppt | ppt | | |
| F19 | | 50 | | | P-407 | 0.2 | 117.40±11.10 | 0.29±0.04 |
| F20 | | | | | | 0.4 | 118.90 ± 17.10 | 0.30±0.06 |
| F21 | | | | | | 0.1 | 493.30±50.00 | 0.50±0.03 |
| F22 | 50 | P-407 | 0.2 | 437.60±32.30 | 0.47±0.05 | | | |
| F23 | | | 0.4 | 365.60±62.50 | 0.42±0.02 | | | |

All formulae were prepared in an ice bath with magnetic stirring at 1000rpm for 15min followed by bath sonication for 45min. ppt: precipitation occurred. ACZ: acetazolamide, PVA: polyvinyl alcohol, P-407: poloxamer 407, S/AS: solvent to anti-solvent ratio.

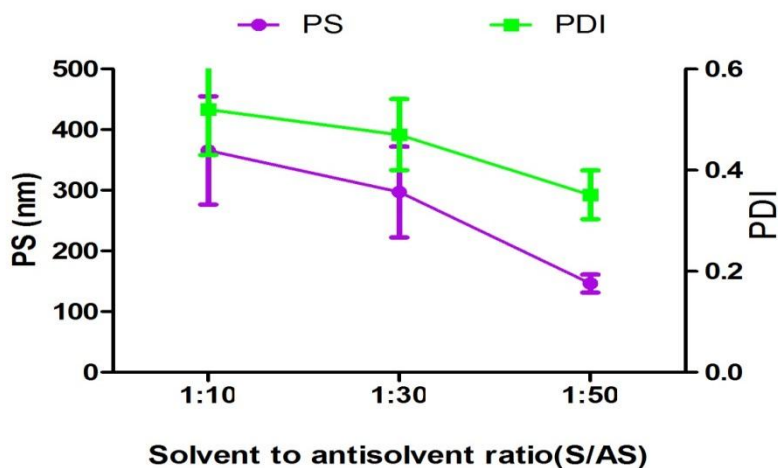


Figure 4: Effect of solvent to the antisolvent ratio (S/AS) on PS and PDI of ACZ-NS.

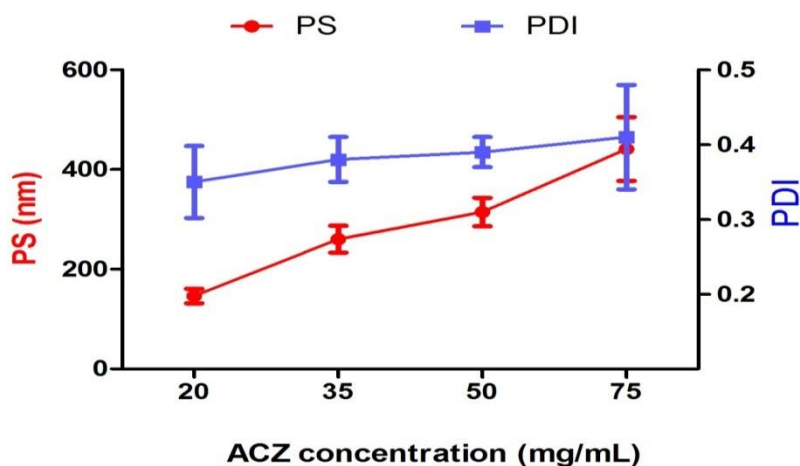


Figure 5: Effect of drug concentration in DMSO on PS and PDI of ACZ-NS.

4.1.5. Effect of type and concentration of stabilizer

Attempts were made to decrease PS of F16 and enhance formulation homogeneity by increasing PVA concentration using 0.2 and 0.4% w/v, in F19 and F20. As illustrated in table 3 and figure 6, both formulae exhibited the same significantly lower PS and PDI. The respective recorded values for PS and PDI were 117.4 ± 11.1 nm, 118.9 ± 17.1 nm and 0.29 ± 0.04 , 0.30 ± 0.06 in comparison to 314.6 ± 28.5 nm and 0.39 ± 0.02 noticed with F16. Consequently, 0.2% w/v PVA was taken as an optimum stabilizer concentration for ACZ-NS.

NS is a thermodynamically unstable system due to the high surface area of small-sized particles [3]. To protect particles against aggregation and growth, different types of stabilizers

that impart either steric or electrostatic stabilization are used to cover particles surface and decrease energy [10]. Hence, P-407 was tried as a steric stabilizer.

P-407 was used at 0.1, 0.2 and 0.4%w/v in formulae F21, F22 and F23, respectively. The three formulae exhibited higher PS and PDI compared to their corresponding counterparts prepared with PVA, table 3 and figure 6. In contrast to NS prepared with PVA, all P-407 stabilized NS showed obvious precipitation one day after preparation (Figure 7).

The poor stabilization power of P-407 might be attributed to its high HLB value (22) [35] compared to PVA (HLB =18) [36]. A polymeric surfactant, by its ability to be adsorbed on the particle surface, creates steric repulsion between particles, thus diminishing particle aggregation and maintaining small PS. At high HLB value, the polymer is more hydrophilic hence, attracted to the aqueous environment leaving particle surface behind. Naked particles become more liable to aggregation and growth [37]. Additionally, SAA with high HLB value is considered as a solubilizer rather than a wetting agent. Drug solubilization worsens NS stability due to Ostwald ripening [38]. Furthermore, Deng and *co-workers* prepared paclitaxel nanocrystals and investigated the effect of P-407 as a stabilizer at a different drug to stabilizer ratios. Unfortunately, whatever the concentration used, P-407 failed to stabilize NS. They ascribed the results to its low CMC value of 7.19×10^{-5} M. At values above CMC, P-407 exhibits lower adsorption affinity to particle surface [39]. It will be present abundantly in the bulk solution forming micelles. Therefore, nanocrystals destabilization occurs forming larger particles [39].

Conversely, PVA seemed to be efficiently adsorbed on the particle surface, creating boundary layer and steric repulsion between particles hindering particles growth and aggregation. Such PVA abilities were previously attributed to hydrogen bond formation between the polymer rich in hydroxyl groups and acetylamino group and sulfonamide groups of ACZ [28, 40], such kind of interaction was reported by literature [41]. In this context, Xia and *co-workers* concluded, that during nitrendipine nanocrystals preparation, an optimum polymer concentration was required for the production of a specific PS. Low polymer concentration was insufficient for surface coating and steric stabilization while high polymer content induced many boundary layers formation accompanied with increasing viscosity which hindered ultrasonic wave transmission and S/AS diffusion [40].

Based on the criteria of attaining the smallest PS and PDI in this group and accordingly F19 was selected for further characterization.

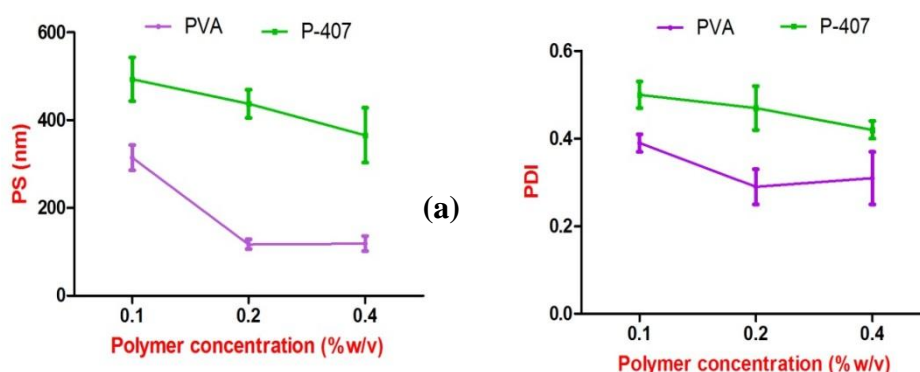


Figure 6: Effect of stabilizer type and concentration on (a) PS and (b) PDI of ACZ-NS.

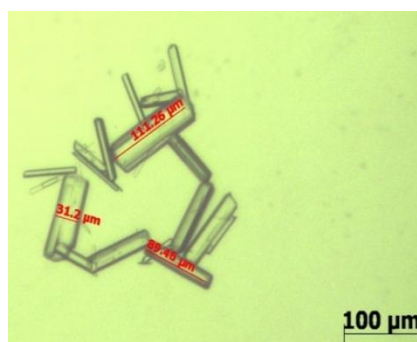


Figure 7: Photomicrograph by optical microscope showing precipitating crystals of P-407 stabilized ACZ-NS 24h following preparation and storage at 4°C.

4.2.Characterization of selected ACZ-NS

F19 shows the optimum required PS of 117.40 ± 11.10 and homogenous PSD manifested by small PDI value of 0.29 ± 0.04 . Hence, it was selected for TEM imaging, solid-state evaluation, and release study.

4.2.1. Microscopical examination of the selected formula

As seen in figure 8, TEM micrographs delineate spherical smooth particles with no sign of agglomeration [42]. Additionally, PS was in range 100-300 nm in accordance with DLS analysis.

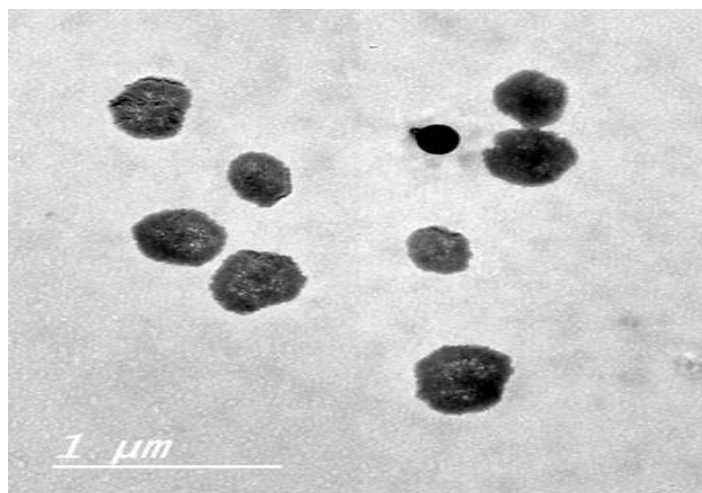


Figure 8: TEM micrograph of ACZ-NS selected formula (F19).

4.2.2. Differential scanning calorimetry (DSC)

In an attempt to investigate the effect of preparation technique (AS-PS) on ACZ crystallinity, the thermal behavior of pure ACZ, excipients and selected formulae was studied using DSC. As seen in figure 9, In accordance with the literature, ACZ exhibits a sharp melting endothermic peak at 271.2°C denoting its crystalline nature, followed by an exothermic transition pointing to its decomposition [43]. Similarly, PVA exhibits a broad melting peak with an onset at 183.8°C, end set at 233.2°C and a peak maximum of 225.2 °C denoting its semi-crystalline nature [44, 45]. Conversely, in F19 thermogram these peaks were not observed hence, suggesting the conversion of crystalline to amorphous into solid solution state during the preparation of nanosuspension [1, 33]. It only shows a sharp endothermic peak below 100°C, which may be due to water evaporation as DSC, was made on liquid formula. Furthermore, the PVA melting peak had disappeared due to the dilution effect and very low stabilizer concentration in the formula [46].

4.2.3. ACZ *in vitro* release

The release profile of ACZ from the developed NS revealed that NS had enhanced drug release compared to a drug suspension. As noted in figure 10, after 5 min about 100 and 37% w/w of NS and drug had been released, respectively. These results may be ascribed to the effect of NS on saturation solubility and dissolution rate. According to the Noyes-Whitney equation, reduction of PS below 1μm produces high surface area to volume ratio thus increasing dissolution rate[47]. Furthermore, according to Kelvin equation reduction of PS

below 1 μ m increases dissolution pressure which depends on particle curvature [48]. Moreover, the amorphization of the drug during nanoprecipitation provided high surface energy due to Gibb's free energy resulting in enhanced saturation solubility and dissolution rate compared to crystalline large drug particle[33, 49].

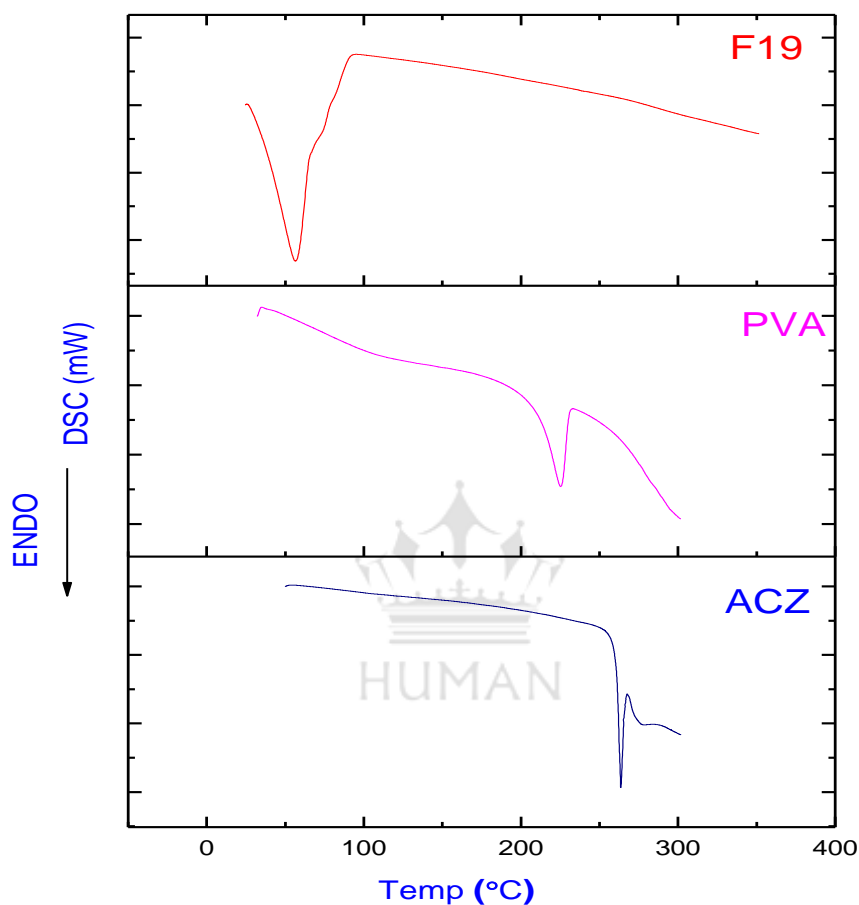


Figure 9: DSC thermograms of ACZ, PVA, and selected formula F19.

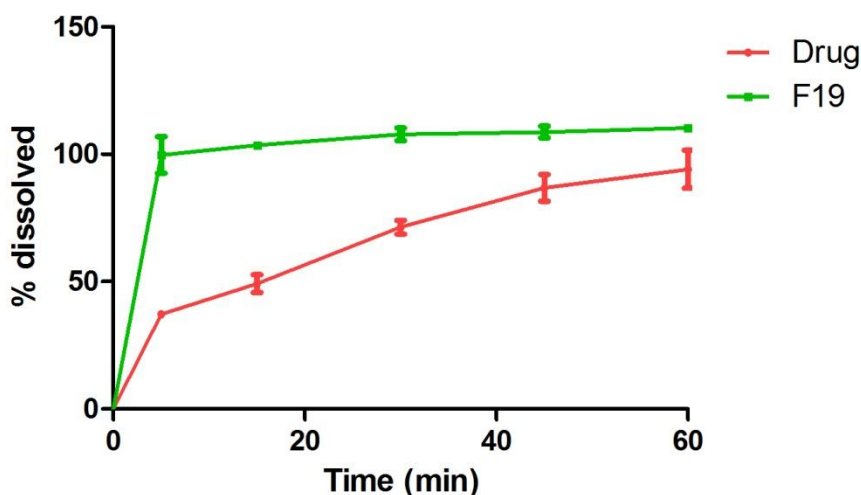


Figure 10: Release profiles of ACZ from its suspension and selected NS formula (F19) in PBS at 37°C.

CONCLUSION

The ultimate goal of this study was to prepare NS of ACZ with optimum PS, homogenous PS distribution with the highest possible drug loading adopting the AS-PT method. A stirring rate of 1000 rpm for 15 min, bath sonication for 45 min while kept in ice bath provided NS with optimum PS and PDI. Moreover, DMSO proved to be a good solvent with an optimum S/AS ratio of 1:50. ACZ concentration in the solvent was critical as very high drug concentration led to system precipitation so, a concentration of 50mg/mL was sufficient to prepare NS with optimum PS and drug loading. Finally, 0.2% w/v PVA provided sufficient steric stabilization that isolated the particles against aggregation. An enhanced release of ACZ from the NS was noted. Amorphization of the particles was demonstrated through TEM and DSC measurements. In the end, optimizing experimental and formulation variables affecting ACZ-NS characteristics prepared using this bottom-up technique; provided a formula showing promising properties for ocular delivery.

REFERENCES

1. Li, Y., et al., Globular protein-coated paclitaxel nanosuspensions: interaction mechanism, direct cytosolic delivery, and significant improvement in pharmacokinetics. *Molecular pharmaceutics*, 2015. 12(5): p. 1485-1500.
2. C Nagarwal, R., et al., Nanocrystal technology in the delivery of poorly soluble drugs: an overview. *Current drug delivery*, 2011. 8(4): p. 398-406.
3. Du, J., et al., Nanosuspensions of poorly water-soluble drugs prepared by bottom-up technologies. *International Journal of Pharmaceutics*, 2015. 495(2): p. 738-749.

4. Tuomela, A., et al., Production, applications and in vivo fate of drug nanocrystals. *Journal of Drug Delivery Science and Technology*, 2016. 34: p. 21-31.
5. Müller, R.H., S. Gohla, and C.M. Keck, State of the art of nanocrystals—special features, production, nanotoxicology aspects and intracellular delivery. *European Journal of Pharmaceutics and Biopharmaceutics*, 2011. 78(1): p. 1-9.
6. Möschwitzer, J.P., Drug nanocrystals in the commercial pharmaceutical development process. *International journal of pharmaceutics*, 2013. 453(1): p. 142-156.
7. Mishra, P.R., et al., Production and characterization of Hesperetin nanosuspensions for dermal delivery. *International Journal of Pharmaceutics*, 2009. 371(1): p. 182-189.
8. Parmentier, J., et al., Downstream drug product processing of itraconazole nanosuspension: Factors influencing drug particle size and dissolution from nanosuspension-layered beads. *International Journal of Pharmaceutics*, 2017. 524(1): p. 443-453.
9. Sinha, B., R.H. Müller, and J.P. Möschwitzer, Bottom-up approaches for preparing drug nanocrystals: Formulations and factors affecting particle size. *International Journal of Pharmaceutics*, 2013. 453(1): p. 126-141.
10. Agarwal, V. and M. Bajpai, Preparation and optimization of esomeprazole nanosuspension using evaporative precipitation—ultrasonication. *Tropical Journal of Pharmaceutical Research*, 2014. 13(4): p. 497-503.
11. Bajaj, A., et al., Nanocrystallization by evaporative antisolvent technique for solubility and bioavailability enhancement of telmisartan. *AAPS PharmSciTech*, 2012. 13(4): p. 1331-1340.
12. Kaur, I.P., et al., Acetazolamide: future perspective in topical glaucoma therapeutics. *International journal of pharmaceutics*, 2002. 248(1-2): p. 1-14.
13. Quinteros, D.A., et al., Novel Polymeric Nanoparticles Intended for Ophthalmic Administration of Acetazolamide. *Journal of Pharmaceutical Sciences*, 2016. 105(10): p. 3183-3190.
14. Mishra, V. and N.K. Jain, Acetazolamide encapsulated dendritic nano-architectures for effective glaucoma management in rabbits. *International Journal of Pharmaceutics*, 2014. 461(1–2): p. 380-390.
15. Guinedi, A.S., et al., Preparation and evaluation of reverse-phase evaporation and multilamellar niosomes as ophthalmic carriers of acetazolamide. *International journal of pharmaceutics*, 2005. 306(1): p. 71-82.
16. Kaur, I., A. Mitra, and D. Aggarwal, Development of a vesicular system for effective ocular delivery of acetazolamide a comprehensive approach and successful venture. *Journal of drug delivery science and technology*, 2007. 17(1): p. 33-41.
17. Lu, Y., et al., Development and evaluation of transferrin-stabilized paclitaxel nanocrystal formulation. *Journal of Controlled Release*, 2014. 176: p. 76-85.
18. Tran, T.T.-D., K.A. Tran, and P.H.-L. Tran, Modulation of particle size and molecular interactions by sonoprecipitation method for enhancing dissolution rate of poorly water-soluble drug. *Ultrasonics Sonochemistry*, 2015. 24: p. 256-263.
19. Tuomela, A., et al., Brinzolamide nanocrystal formulations for ophthalmic delivery: Reduction of elevated intraocular pressure in vivo. *International Journal of Pharmaceutics*, 2014. 467(1–2): p. 34-41.
20. Rathod, L.V., R. Kapadia, and K.K. Sawant, A novel nanoparticles impregnated ocular insert for enhanced bioavailability to posterior segment of eye: In vitro, in vivo and stability studies. *Materials Science and Engineering: C*, 2017. 71: p. 529-540.
21. D'Addio, S.M. and R.K. Prud'homme, Controlling drug nanoparticle formation by rapid precipitation. *Advanced Drug Delivery Reviews*, 2011. 63(6): p. 417-426.
22. Parasrampur, J., Acetazolamide, in *Analytical Profiles of Drug Substances and Excipients*, H.G. Brittain, Editor. 1993, Academic Press. p. 1-32.
23. Pu, X., et al., Development of a chemically stable 10-hydroxycamptothecin nanosuspensions. *International Journal of Pharmaceutics*, 2009. 379(1): p. 167-173.
24. Griesser, U.J., A. Burger, and K. Mereiter, The polymorphic drug substances of the European Pharmacopoeia. Part 9. Physicochemical properties and crystal structure of acetazolamide crystal forms. *Journal of pharmaceutical sciences*, 1997. 86(3): p. 352-358.
25. Matteucci, M.E., et al., Drug Nanoparticles by Antisolvent Precipitation: Mixing Energy versus Surfactant Stabilization. *Langmuir*, 2006. 22(21): p. 8951-8959.

26. Dalvi, S.V. and R.N. Dave, Controlling Particle Size of a Poorly Water-Soluble Drug Using Ultrasound and Stabilizers in Antisolvent Precipitation. *Industrial & Engineering Chemistry Research*, 2009. 48(16): p. 7581-7593.
27. Murnane, D., C. Marriott, and G.P. Martin, Developing an environmentally benign process for the production of microparticles: Amphiphilic crystallization. *European Journal of Pharmaceutics and Biopharmaceutics*, 2008. 69(1): p. 72-82.
28. Mishra, B., J. Sahoo, and P.K. Dixit, Formulation and process optimization of naproxen nanosuspensions stabilized by hydroxy propyl methyl cellulose. *Carbohydrate Polymers*, 2015. 127(Supplement C): p. 300-308.
29. Kitayama, H., et al., A common mechanism underlying amyloid fibrillation and protein crystallization revealed by the effects of ultrasonication. *Biochimica et Biophysica Acta (BBA) - Proteins and Proteomics*, 2013. 1834(12): p. 2640-2646.
30. Anup, N., S. Thakkar, and M. Misra, Formulation of olanzapine nanosuspension based orally disintegrating tablets (ODT); comparative evaluation of lyophilization and electrospraying process as solidification techniques. *Advanced Powder Technology*, 2018. 29(8): p. 1913-1924.
31. Shariare, M.H., et al., The impact of process parameters on carrier free paracetamol nanosuspension prepared using different stabilizers by antisolvent precipitation method. *Journal of Drug Delivery Science and Technology*, 2018. 43: p. 122-128.
32. Singh, M.K., et al., Fabrication of surfactant-stabilized nanosuspension of naringenin to surpass its poor physiochemical properties and low oral bioavailability. *Phytomedicine*, 2018. 40: p. 48-54.
33. Kumar, S., J. Shen, and D.J. Burgess, Nano-amorphous spray dried powder to improve oral bioavailability of itraconazole. *Journal of Controlled Release*, 2014. 192(Supplement C): p. 95-102.
34. Sahu, B.P. and M.K. Das, Nanoprecipitation with sonication for enhancement of oral bioavailability of furosemide. *Acta Poloniae Pharmaceutica N Drug Research*, 2014. 71(1): p. 129-137.
35. Malamatarı, M., et al., Nanoparticle agglomerates of indomethacin: the role of poloxamers and matrix former on their dissolution and aerosolisation efficiency. *International journal of pharmaceutics*, 2015. 495(1): p. 516-526.
36. Xu, Q., A. Crossley, and J. Czernuszka, Preparation and characterization of negatively charged poly (lactic-co-glycolic acid) microspheres. *Journal of pharmaceutical sciences*, 2009. 98(7): p. 2377-2389.
37. Verma, S., R. Gokhale, and D.J. Burgess, A comparative study of top-down and bottom-up approaches for the preparation of micro/nanosuspensions. *International Journal of Pharmaceutics*, 2009. 380(1): p. 216-222.
38. Kumar, S., et al., Formulation and performance of danazol nano-crystalline suspensions and spray dried powders. *Pharmaceutical research*, 2015. 32(5): p. 1694-1703.
39. Deng, J., L. Huang, and F. Liu, Understanding the structure and stability of paclitaxel nanocrystals. *International Journal of Pharmaceutics*, 2010. 390(2): p. 242-249.
40. Xia, D., et al., Preparation of stable nitrendipine nanosuspensions using the precipitation-ultrasonication method for enhancement of dissolution and oral bioavailability. *European Journal of Pharmaceutical Sciences*, 2010. 40(4): p. 325-334.
41. Douromis, D. and A. Fahr, Stable carbamazepine colloidal systems using the cosolvent technique. *European Journal of Pharmaceutical Sciences*, 2007. 30(5): p. 367-374.
42. Ambhore, N.P., P.M. Dandagi, and A.P. Gadad, Formulation and comparative evaluation of HPMC and water soluble chitosan-based sparfloxacin nanosuspension for ophthalmic delivery. *Drug Delivery and Translational Research*, 2016. 6(1): p. 48-56.
43. Mora, M.J., et al., Characterization, dissolution and in vivo evaluation of solid acetazolamide complexes. *Carbohydrate polymers*, 2013. 98(1): p. 380-390.
44. Parparita, E., C.N. Cheaburu, and C. Vasile, Morphological, thermal and rheological characterization of polyvinyl alcohol/chitosan blends. *Cellulose Chemistry and Technology*, 2012. 46(9-10): p. 571-581.
45. Jelinska, N., et al., Poly (vinyl alcohol)/poly (vinyl acetate) blend films. *Sci. J. of Riga Techn. Univ., Mater. Sci. Appl. Chem*, 2010. 1: p. 55-61.
46. Thadkala, K., et al., Preparation and characterization of amorphous ezetimibe nanosuspensions intended for enhancement of oral bioavailability. *International journal of pharmaceutical investigation*, 2014. 4(3): p. 131.
47. Noyes, A.A. and W.R. Whitney, The rate of solution of solid substances in their own solutions. *Journal of the American Chemical Society*, 1897. 19(12): p. 930-934.

48. Shegokar, R. and R.H. Müller, Nanocrystals: industrially feasible multifunctional formulation technology for poorly soluble actives. *International Journal of Pharmaceutics*, 2010. 399(1): p. 129-139.
49. Leuner, C. and J. Dressman, Improving drug solubility for oral delivery using solid dispersions. *European journal of Pharmaceutics and Biopharmaceutics*, 2000. 50(1): p. 47-60.

